

Phase transitions in a spin-1 model with plaquette interaction on the square lattice

Original

Phase transitions in a spin-1 model with plaquette interaction on the square lattice / Buzano, Carla; L. R., Evangelista; Pelizzola, Alessandro. - In: PHYSICAL REVIEW. B, CONDENSED MATTER. - ISSN 0163-1829. - 53:(1996), pp. 15063-15070. [10.1103/PhysRevB.53.15063]

Availability:

This version is available at: 11583/1397838 since:

Publisher:

APS

Published

DOI:10.1103/PhysRevB.53.15063

Terms of use:

This article is made available under terms and conditions as specified in the corresponding bibliographic description in the repository

Publisher copyright

(Article begins on next page)

Phase transitions in a spin-1 model with plaquette interaction on the square lattice

C. Buzano

*Dipartimento di Fisica del Politecnico di Torino and Istituto Nazionale di Fisica della Materia,
Corso Duca degli Abruzzi 24, 10129 Torino, Italy*

L. R. Evangelista

*Dipartimento di Fisica del Politecnico di Torino and Istituto Nazionale di Fisica della Materia,
Corso Duca degli Abruzzi 24, 10129 Torino, Italy
and Departamento de Física, Universidade Estadual de Maringá, Avenida Colombo, 5790 Maringá, Paraná, Brazil*

A. Pelizzola

*Dipartimento di Fisica del Politecnico di Torino and
Istituto Nazionale di Fisica della Materia, Corso Duca degli Abruzzi 24, 10129 Torino, Italy*

(Received 10 November 1995; revised manuscript received 12 January 1996)

An extension of the Blume-Emery-Griffiths model with a plaquette four-spin interaction term, on the square lattice, is investigated by means of the cluster variation method in the square approximation. The ground state of the model, for negative plaquette interaction, exhibits several new phases, including frustrated ones. At finite temperature we obtain a quite rich phase diagram with two new phases, a ferrimagnetic and a weakly ferromagnetic one, and several multicritical points. [S0163-1829(96)04222-1]

I. INTRODUCTION

The spin-1 Ising model with a bilinear and biquadratic nearest-neighbor interaction, the Blume-Emery-Griffiths (BEG) model, has attracted a great deal of attention since it was originally proposed to describe phase separation and superfluid ordering in ^3He - ^4He mixtures.¹ It has subsequently been used to describe the properties of several systems ranging from multicomponent fluids,² microemulsions,³ semiconductor alloys,⁴ and electronic conduction models⁵ to reentrant behavior of lyotropic nematic liquid crystals.⁶ It is just the richness of its phase diagram that is one of the main reasons for this interest. In fact, the system has been studied by a variety of techniques: the mean field approximation,^{1,7-9} high-temperature series expansion,¹⁰ Monte Carlo methods,^{11,12} renormalization group,¹³⁻²⁰ effective field theory,²¹⁻²³ and cluster variation method²⁴⁻²⁷ among others. Recently, it has been shown that the global phase diagram of this system includes nine distinct topologies and three ordered phases,⁹ with the appearance of ferrimagnetic phases for a certain range of coupling parameters.²⁵ The occurrence of a reentrance in the ferromagnetic-paramagnetic transition has been also pointed out by some authors.^{19,21-24,27}

In this paper we shall investigate, in the framework of the square approximation of the cluster variation method (CVM),²⁸⁻³⁰ an extension of the square lattice BEG model, which includes a four-spin (plaquette) quadrilinear interaction term, in order to analyze the thermodynamic of the frustrated phases which arise in this case. Such phases may be obtained also by including next-nearest-neighbor interactions, but in this case it is necessary to introduce both a bilinear and a biquadratic coupling, thus increasing the dimensionality of the parameter space by 2. The four-spin interaction has then the advantage to allow us to obtain frus-

trated ground states in a smaller parameter space. In this sense the model we propose can be regarded as a minimal model for such phases.

The CVM is an approximate variational technique for the treatment of cooperative phenomena and has been successfully applied to study the critical behavior of spin-1 models.²⁴⁻²⁷ It is especially suited for the analysis of complex phase diagrams since the order of a phase transition can be easily recognized and order parameters, local correlation functions, and the free energy are readily obtained. The accuracy of the approximation can be systematically improved by increasing the basic clusters. On a square lattice, however, the square approximation is in most cases sufficient to obtain a qualitatively correct phase diagram and also quite good approximations for numerical results.

The main purpose of our work is to analyze the effect of the plaquette interaction term on the phase diagram of the BEG model, paying particular attention to the case of a negative plaquette interaction. A negative plaquette interaction introduces frustration effects which result in an infinite degeneracy of the ground state, although the entropy per site still vanishes in the limit of zero temperature. At finite temperature some interesting effects appear, such as two new phases, a ferrimagnetic and a weakly ferromagnetic one, uncommon behaviors in the order parameters, and several multicritical points.

Our paper is organized as follows. In Sec. II the model is presented and the free energy of the system is written in the CVM square approximation. Section III is devoted to the analysis of ground-state configurations. In Sec. IV the equations for the critical temperature are determined. In Sec. V we discuss the finite-temperature phase diagram and the results of CVM square calculations for the model. Some concluding remarks are presented in Sec. VI.

II. MODEL AND THE CVM FREE ENERGY

We consider a spin-1 model (composed of a bilinear interaction, a biquadratic interaction, and crystal-field terms) with a four-body interaction term, in the form

$$H = -J \sum_{\langle ij \rangle} S_i S_j - K \sum_{\langle ij \rangle} S_i^2 S_j^2 + D \sum_i S_i^2 - G \sum_{\langle ijkl \rangle} S_i S_j S_k S_l, \quad (2.1)$$

where S_i is the z component of a spin-1 operator at site i of a square lattice. $\sum_{\langle ij \rangle}$ indicates summation over all nearest neighbors, $\sum_{\langle ijkl \rangle}$ indicates summation over four sites in the square (plaquette), and $J > 0$. The above model reduces to the Blume-Emery-Griffiths (BEG) model¹ when $G=0$ and to the Blume-Capel^{32,33} (BC) model for $K=0$ and $G=0$. Notice also that, in the limit of an extreme negative crystal field, our model reduces to the well-known Ising model with a plaquette interaction (see, e.g., Ref. 31).

We shall analyze the phase transitions of the model in the square approximation of the cluster variation method (CVM). In the CVM the entropy of the system is approximated as a sum of suitably weighted cluster entropies relative to a set Γ of maximal clusters and of all their subclusters,²⁹

$$S = \sum_{\sigma \in \Gamma} a_\sigma N_\sigma S_\sigma, \quad (2.2)$$

where

$$S_\sigma = -k_B \text{Tr}(\rho_\sigma \ln \rho_\sigma) \quad (2.3)$$

is the entropy associated with the cluster σ . In the above equations, k_B is the Boltzmann constant, T the absolute temperature, N_σ is the total number of clusters of the σ kind, a_σ is a counting factor, which can be calculated using Moebius inversion,²⁹ and ρ_σ is the reduced density matrix for cluster σ .

The free energy per site f is then written as

$$f = \sum_{\sigma \in \Gamma} \frac{N_\sigma}{N} [\text{Tr}(\rho_\sigma H_\sigma) + k_B T a_\sigma \text{Tr}(\rho_\sigma \ln \rho_\sigma)], \quad (2.4)$$

where H_σ is the n_σ -body interaction contribution associated with the cluster σ (the maximal clusters should be taken large enough to contain all kind of interactions present in H).

According to the CVM, the free energy f will be minimized with respect to the density matrices ρ_σ , with the constraints

$$\text{Tr} \rho_\sigma = 1, \quad \rho_\sigma = \text{Tr}_{\eta \setminus \sigma} \rho_\eta, \quad \eta > \sigma, \quad (2.5)$$

$\text{Tr}_{\eta \setminus \sigma}$ denoting a partial trace.

In the CVM square approximation, the entropy will be the sum of contributions of one-site clusters, two-site clusters, and four-site clusters, and the free energy will take the form

$$\begin{aligned} f = & \text{Tr}(\rho_4 H_4) + k_B T \left[\frac{1}{4} \text{Tr}(\rho_1^i \ln \rho_1^i) + \frac{1}{4} \text{Tr}(\rho_1^j \ln \rho_1^j) \right. \\ & + \frac{1}{4} \text{Tr}(\rho_1^k \ln \rho_1^k) + \frac{1}{4} \text{Tr}(\rho_1^l \ln \rho_1^l) - \frac{1}{2} \text{Tr}(\rho_2^{ij} \ln \rho_2^{ij}) \\ & - \frac{1}{2} \text{Tr}(\rho_2^{jk} \ln \rho_2^{jk}) - \frac{1}{2} \text{Tr}(\rho_2^{kl} \ln \rho_2^{kl}) - \frac{1}{2} \text{Tr}(\rho_2^{li} \ln \rho_2^{li}) \\ & \left. + \text{Tr}(\rho_4 \ln \rho_4) \right]. \quad (2.6) \end{aligned}$$

In Eq. (2.6) we have considered four sublattices. The labels 1, 2, and 4 refer, respectively, to site, pair, and square density matrices, while i, j, k, l label the sublattices (and the sites of the plaquette belonging to them) of the square cluster [$i-j, j-k, k-l, l-i$ are nearest-neighbor (NN) sites]. Moreover,

$$\begin{aligned} H_4 = & -\frac{J}{2} [(S_i + S_k)(S_j + S_l)] + \frac{D}{4} [S_i^2 + S_j^2 + S_k^2 + S_l^2] \\ & - \frac{K}{2} [(S_i^2 + S_k^2)(S_j^2 + S_l^2)] - G [S_i S_j S_k S_l]. \quad (2.7) \end{aligned}$$

Taking into account the constraints, Eq. (2.5), the free energy f can be considered as a function of the elements of the square density matrix only, obeying the condition $\text{Tr} \rho_4 = 1$.

Looking for a stationary point one obtains the equations

$$\rho_4(s_i, s_j, s_k, s_l) = r_4(s_i, s_j, s_k, s_l) e^{-\beta H_4(s_i, s_j, s_k, s_l)} e^{-\beta \lambda}, \quad (2.8)$$

where $\beta = 1/k_B T$,

$$\begin{aligned} r_4(s_i, s_j, s_k, s_l) = & \frac{[\rho_2^{ij}(s_i, s_j) \rho_2^{jk}(s_j, s_k) \rho_2^{kl}(s_k, s_l) \rho_2^{li}(s_l, s_i)]^{1/2}}{[\rho_1^i(s_i) \rho_1^j(s_j) \rho_1^k(s_k) \rho_1^l(s_l)]^{1/4}}, \quad (2.9) \end{aligned}$$

and

$$e^{\beta \lambda} = \sum_{s_i, s_j, s_k, s_l} r_4(s_i, s_j, s_k, s_l) e^{-\beta H_4(s_i, s_j, s_k, s_l)}. \quad (2.10)$$

In Eqs. (2.8)–(2.10), s_i, s_j, s_k, s_l are the eigenvalues of the spin-1 operators at site i, j, k, l and can take the values $-1, 0, 1$. They have been used to label the diagonal density matrix elements.

Equations (2.8) can be solved by using the natural iteration method.³⁴ It is possible to show that the solutions obtained by this method are always local minima of f . When f has many local minima, these can be determined by choosing several different guess values for the iteration; the solution will be the one which minimizes the free energy f .

Once Eqs. (2.8) are solved, we can easily determine the dipolar $m^{(r)}$ ($r = i, j, k, l$) and quadrupolar $q^{(r)}$ order parameters in each sublattice by

$$\begin{aligned}
m^{(r)} &= \langle S_r \rangle = \rho_1^r(+1) - \rho_1^r(-1), \\
q^{(r)} &= \langle S_r^2 \rangle = \rho_1^r(+1) + \rho_1^r(-1), \quad r=i, j, k, l,
\end{aligned}
\tag{2.11}$$

as well as the two-site NN and four-site (plaquette) correlations ($\langle \dots \rangle$ means thermal average).

III. GROUND STATE

In this section we shall consider the ground-state configurations of the spin-1 model introduced above. The ground state of an Ising-like spin model can be easily determined, in the cluster variation method, by looking for the configurations of the maximal clusters which minimize the free energy at $T=0$, that is, the internal energy. The results so obtained are exact provided the exact ground state is homogeneous; i.e., it can be obtained by indefinitely repeating a unique local ground-state for a cluster equal to, or smaller than, a maximal cluster.

In the present approximation scheme a configuration of the maximal cluster is specified by the eigenvalues of the four spin-1 operators lying on a square, and is denoted by $\{s_i, s_j, s_k, s_l\}$, where the indices refer to the four sublattices previously introduced.

Among the possible ground-state configurations we shall certainly have those of the usual Blume-Emery-Griffiths model, i.e., the ferromagnetic state $\{1,1,1,1\}$ (or $\{-1, -1, -1, -1\}$ as well), which will be denoted by F , the paramagnetic (P) state $\{0,0,0,0\}$, and the so-called antiquadrupolar or staggered quadrupolar (Q) state $\{0, \pm 1, 0, \pm 1\}$. In the Q state, all the spins belonging to two non-nearest-neighbor sublattices (j and l or i and k) can take on the values 1 and -1 independently and with the same probability. Given an $N \times M$ lattice there are $2^{NM/2}$ such states and thus we have a $T=0$ entropy per site which, in the thermodynamic limit, equals $\frac{1}{2} \ln 2$, exactly reproduced by our approximation. In terms of the square density matrix this state is characterized by $\rho_4(s_i, s_j, s_k, s_l) = 1/4$ if $s_i = s_k = 0$ and $|s_j| = |s_l| = 1$ and zero otherwise.

In addition, having introduced a plaquette interaction which can take on negative values, we shall consider, in order to take into account all the possible minima of the internal energy, also the local ground states E , given by $\{1, 0, 1, 1\}$ (with degeneracy 8, since the zero spin can be in any sublattice and the three nonzero spins can be either 1 or -1), and S , given by $\{1, -1, 1, 1\}$ (again with degeneracy 8).

It is easily recognized that the local ground states E and S correspond to inhomogeneous, highly degenerate, global ground states. To begin with, let us consider the local ground state E and try to construct a global ground state in which all the elementary plaquettes are in the state E , an example being reported in Fig. 1. We have two sublattices (say, k and l) which are occupied by $+$ spins only, while the other two (i and j) are occupied by $+$ and 0 spins. The relative concentrations of $+$ and 0 spins can be different in the two sublattices i and j , but are always equal if the two sublattices are taken as a whole. On the average, however, $+$ and 0 will be evenly distributed. Furthermore, two adjacent basic lines (columns in Fig. 1) are indefinitely repeated with a period equal to two lattice constants. The degeneracy of such a state, for a lattice with N rows and M columns, is

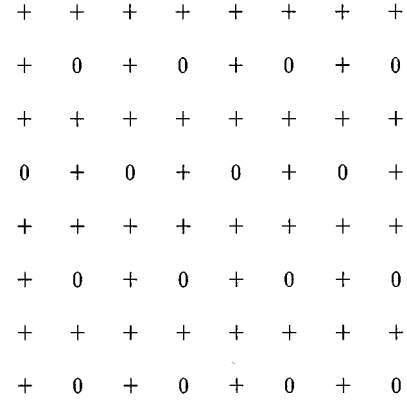


FIG. 1. An example of the E ground state.

$2^{N/2} + 2^{M/2}$, which in the thermodynamic limit yields a vanishing entropy per site, again reproduced exactly by our approximation.

The case of the S local ground state is somewhat more involved because $+$ and $-$ spins can coexist in the same plaquette and hence one may ask whether the $+/-$ (spin flip) symmetry is broken or not in the global ground state. If the symmetry is broken, the only plaquettes available to build up the local ground state are, e.g., those with three $+$ spins and one $-$ spin, and the global ground state can be obtained from the E one by replacing all the 0 spins with $-$ spins. We shall denote this case by A from now on. If the spin-flip symmetry is preserved, the global ground state is made up of plaquettes which satisfy the condition

$$s_i s_j s_k s_l = -1, \tag{3.1}$$

and an example is shown in Fig. 2. In this case one can choose freely the value ($+$ or $-$) of all the spins in a given row and a given column, and the remaining spins are determined by Eq. (3.1). The degeneracy is then 2^{N+M-1} and again the entropy per site vanishes in the thermodynamic limit, as our approximation predicts.

In order to determine which state is the ground state in a given point of the $T=0$ phase space we have computed the internal energy per site $e = \text{Tr}(\rho_4 H_4)$ of each state, obtaining

$$e_F = D - 2K - 2J - G, \tag{3.2}$$

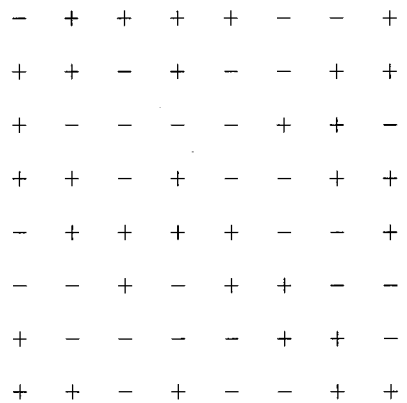


FIG. 2. An example of the S ground state.

$$\begin{aligned}
e_P &= 0, \\
e_Q &= \frac{D}{2}, \\
e_E &= \frac{3}{4}D - K - J, \\
e_A &= D - 2K + G, \\
e_S &= D - 2K + G.
\end{aligned}$$

The boundary between the different phases can be easily obtained by looking for the minimum of the energies above, except for the A/S boundary, since $e_A = e_S$. In this case one has to determine and compare the first terms of the low-temperature expansions of the free energies of the two phases.

For the S phase, it is easily recognized (e.g., by numerical inspection) that the first excitations above the ground state are the F -like local states. The square density matrix at infinitesimal temperature will be given by

$$\begin{aligned}
\rho_4(s_i, s_j, s_k, s_l) &= \frac{1 - \varepsilon_S}{8} \quad \text{if } s_i s_j s_k s_l = -1, \\
\rho_4(s_i, s_j, s_k, s_l) &= \frac{\varepsilon_S}{2} \quad \text{if } s_i = s_j = s_k = s_l = \pm 1, \quad (3.3)
\end{aligned}$$

with ε_S infinitesimal and the remaining elements negligible with respect to ε_S . The free energy, Eq. (2.6), then takes the form

$$\begin{aligned}
f_S &= -2K + D + G - 2\varepsilon_S(J + G) + k_B T \left[8\mathcal{L}\left(\frac{1 - \varepsilon_S}{8}\right) \right. \\
&\quad \left. + 2\mathcal{L}\left(\frac{\varepsilon_S}{2}\right) - 4\mathcal{L}\left(\frac{1 - \varepsilon_S}{4}\right) - 4\mathcal{L}\left(\frac{1 + \varepsilon_S}{4}\right) - \ln 2 \right], \quad (3.4)
\end{aligned}$$

where $\mathcal{L}(x) = x \ln x$. Minimizing with respect to ε_S one finds $\varepsilon_S = \frac{1}{4} \exp[\beta(2J + 2G)]$, and then

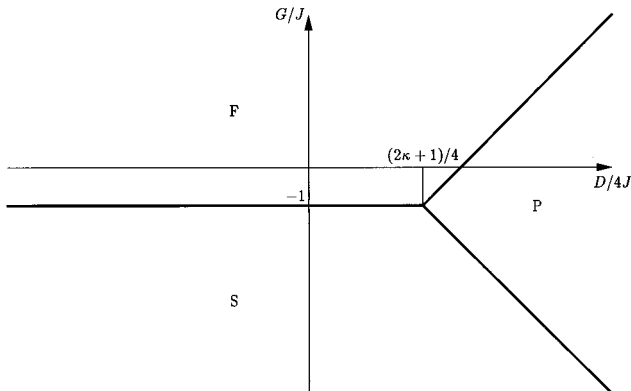


FIG. 3. Ground-state phase diagram for $\kappa = K/J > 1/2$. The F/P phase boundary is given by $G = D - 2K - 2J$ and the S/P one by $G = -D + 2K$.

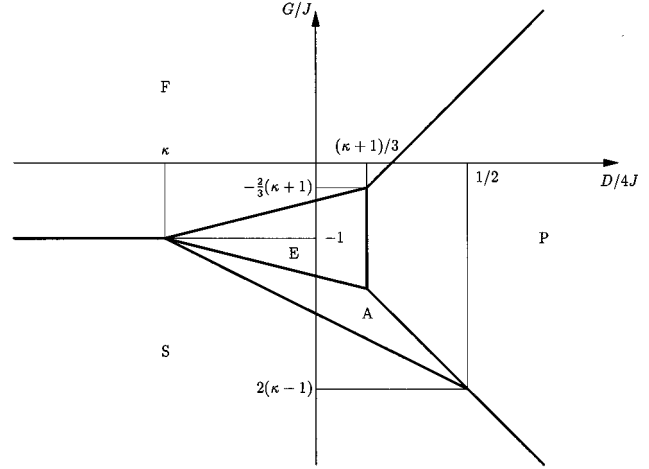


FIG. 4. Ground-state phase diagram for $-1 < \kappa < 1/2$.

$$f_S = -2K + D + G - k_B T \varepsilon_S + \dots \quad (3.5)$$

For the A phase one sees that the first interactions above the ground state are obtained replacing the $-$ spins of the ground state with zero spins. The square density matrix at very low temperature is then

$$\begin{aligned}
\rho_4(1, 1, 1, -1) &= \rho_4(1, 1, -1, 1) = \frac{1 - \varepsilon_A}{2}, \\
\rho_4(1, 1, 1, 0) &= \rho_4(1, 1, 0, 1) = \frac{\varepsilon_A}{2}, \quad (3.6)
\end{aligned}$$

where again ε_A is infinitesimal and the remaining elements are negligible with respect to ε_A . The free energy now becomes

$$\begin{aligned}
f_A &= -2K + D + G + \varepsilon_A(-J + K - D/4 - G) \\
&\quad + k_B T \left[\frac{1}{2} \mathcal{L}\left(\frac{1 - \varepsilon_A}{2}\right) + \frac{1}{2} \mathcal{L}\left(\frac{\varepsilon_A}{2}\right) + \frac{1}{4} \ln 2 \right], \quad (3.7)
\end{aligned}$$

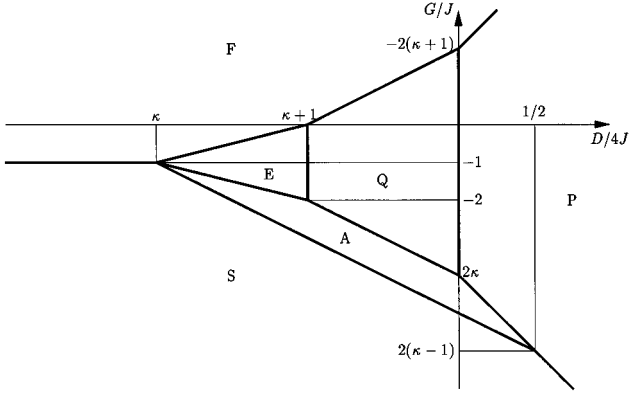
which, minimized with respect to ε_A , yields $\varepsilon_A = \exp[\beta(4J - 4K + D + 4G)]$ and

$$f_A = -2K + D + G - \frac{1}{4} k_B T \varepsilon_A + \dots \quad (3.8)$$

Comparing Eq. (3.5) with Eq. (3.8) one sees that the transition between the S and the A phases takes place for $G = -D/2 + 2K - J$. Reporting on the same plane this transition line together with those obtained by simple comparison of internal energies we have obtained three possible topologies for the ground-state phase diagram at constant $\kappa = K/J$, which are reported in Figs. 3–5.

For $\kappa > 1/2$ (Fig. 3) we find only three ground states, F , P , and S . The unique substantial modification with respect to the ordinary BEG model is the replacement of the F ground state with the S one (which, however, turns into a ferromagneticlike phase at finite temperature) for $G/J < -1$.

For $-1 < \kappa < 1/2$ (Fig. 4) the E and A ground states appear, actually breaking the sublattice invariance. It is on

FIG. 5. Ground-state phase diagram for $\kappa < -1$.

these regions of the phase diagram that most of our attention will concentrate in the following.

Finally, for $\kappa < -1$ (Fig. 5) the antiquadrupolar Q ground state also appears. The antiquadrupolar phase is well known from the study of the ordinary BEG model and we shall almost completely disregard it, since here we are mainly concerned with the effects due to the plaquette interaction term. Our approximation scheme, however, does not need any modification in order to take into account also this phase.

IV. CRITICAL TEMPERATURE

In order to determine the temperature phase diagram it is useful to obtain explicitly the equation for the critical temperature of the ferromagnetic-paramagnetic transition. Since in this case no sublattices are to be introduced, only two order parameters m and q ($m = m^{(r)}$, $q = q^{(r)}$, $r = i, j, k, l$) and three two-site NN correlations $c_1 = \langle S_i S_j \rangle$, $c_2 = \langle S_i^2 S_j^2 \rangle$, $c_x = \langle S_i S_j^2 \rangle$ are to be considered. They can be written in terms of the square density matrix elements as

$$\begin{aligned}
 m &= \sum_{s_i, s_j, s_k, s_l} s_i \rho_4(s_i, s_j, s_k, s_l), \\
 q &= \sum_{s_i, s_j, s_k, s_l} s_i^2 \rho_4(s_i, s_j, s_k, s_l), \\
 c_1 &= \sum_{s_i, s_j, s_k, s_l} s_i s_j \rho_4(s_i, s_j, s_k, s_l), \\
 c_2 &= \sum_{s_i, s_j, s_k, s_l} s_i^2 s_j^2 \rho_4(s_i, s_j, s_k, s_l), \\
 c_x &= \sum_{s_i, s_j, s_k, s_l} s_i s_j^2 \rho_4(s_i, s_j, s_k, s_l). \quad (4.1)
 \end{aligned}$$

Inserting Eq. (2.8) into Eq. (4.1) and considering that the site and pair density matrix elements can be easily expressed as linear combinations of m , q , c_1 , c_2 , and c_x ,²⁶ we obtain five equations in the variables m, q, c_1, c_2, c_x . The critical temperature is evaluated by considering the limit $m \rightarrow 0$. We obtain the following equation for the critical temperature

$$\begin{aligned}
 &\left(W_0 + \frac{L_1}{2\bar{q}} - \frac{L_2}{\bar{q} - \bar{c}_2} \right) \left(W_0 - \frac{L_3}{\bar{c}_1 + \bar{c}_2} + \frac{L_4}{\bar{q} - \bar{c}_2} \right) \\
 &+ \left(\frac{L_4}{\bar{q} - \bar{c}_2} - \frac{L_5}{\bar{q}} \right) \left(\frac{L_2}{\bar{q} - \bar{c}_2} - \frac{4L_5}{\bar{c}_1 + \bar{c}_2} \right) = 0, \quad (4.2)
 \end{aligned}$$

where, for compactness, we have introduced several quantities which will be defined in the sequel, and \bar{q} , \bar{c}_1 , and \bar{c}_2 are the values q , c_1 , and c_2 for $m \rightarrow 0$. These quantities are

$$\begin{aligned}
 L_1 &= 4\gamma_1 a_1 + 9\gamma_2 a_2 + 4\gamma_3 a_3 + 2\gamma_4 a_4 + 4\gamma_5 a_5 \\
 &+ \gamma_6 a_6 + 2\gamma_7 a_7 + \gamma_8 a_8,
 \end{aligned}$$

$$L_2 = 6\gamma_2 a_2 + 4\gamma_5 a_5 + 2\gamma_6 a_6 + 4\gamma_7 a_7 + 2\gamma_8 a_8,$$

$$L_3 = 8\gamma_1 a_1 + 8\gamma_2 a_2 + 8\gamma_3 a_3 + 4\gamma_4 a_4 + 2\gamma_5 a_5,$$

$$L_4 = 4\gamma_2 a_2 + 2\gamma_5 a_5,$$

$$L_5 = 2\gamma_1 a_1 + 3\gamma_2 a_2 + 2\gamma_3 a_3 + \gamma_4 a_4 + \gamma_5 a_5,$$

$$\begin{aligned}
 W_0 &= 2\gamma_1 a_1 + 8\gamma_2 a_2 + 8\gamma_3 a_3 + 16\gamma_4 a_4 + 8\gamma_5 a_5 + 8\gamma_6 a_6 \\
 &+ 8\gamma_7 a_7 + 8\gamma_8 a_8 + 8\gamma_9 a_9 + 4\gamma_{10} a_{10} + 2\gamma_{11} a_{11} + a_{12}, \quad (4.3)
 \end{aligned}$$

where

$$\begin{aligned}
 a_1 &= \eta^2, \quad a_2 = \eta\omega, \quad a_3 = \eta\zeta, \quad a_4 = (\eta\zeta)^{1/2}\omega, \\
 a_5 &= (\eta\tau)^{1/2}\omega, \quad a_6 = \zeta\omega, \quad a_7 = \omega^2, \quad a_8 = \tau\omega, \\
 a_9 &= (\zeta\tau)^{1/2}\omega, \quad a_{10} = \eta\zeta, \quad a_{11} = \zeta^2, \quad a_{12} = \tau^2, \quad (4.4)
 \end{aligned}$$

with

$$\begin{aligned}
 \eta &= \frac{\bar{c}_2 + \bar{c}_1}{(8\bar{q})^{1/2}}, \quad \zeta = \frac{\bar{c}_2 - \bar{c}_1}{(8\bar{q})^{1/2}}, \quad \tau = \frac{1 + \bar{c}_2 - 2\bar{q}}{(1 - \bar{q})^{1/2}}, \\
 \omega &= \frac{\bar{q} - \bar{c}_2}{(8\bar{q}(1 - \bar{q}))^{1/4}}. \quad (4.5)
 \end{aligned}$$

The parameters of the model enter expression Eq. (4.3) by means of the functions γ_i , $i = 1, \dots, 11$, introduced above and defined as

$$\begin{aligned}
 \gamma_1 &= e^{\beta(-D+2J+2K+G)}, \quad \gamma_2 = e^{\beta(-3D/4+J+K)}, \\
 \gamma_3 &= e^{\beta(-D+2K-G)}, \quad \gamma_4 = e^{\beta(-3D/4+K)}, \\
 \gamma_5 &= e^{\beta(-D+J+K)/2}, \\
 \gamma_6 &= e^{\beta(-3D/4-J+K)}, \\
 \gamma_7 &= e^{\beta(-D/2)}, \quad \gamma_8 = e^{\beta(-D/4)}, \\
 \gamma_9 &= e^{\beta(-D-J+K)/2}, \quad \gamma_{10} = e^{\beta(-D+2K+G)}, \\
 \gamma_{11} &= e^{\beta(-D-2J+2K+G)}. \quad (4.6)
 \end{aligned}$$

The quadrupolar order parameter \bar{q} and the correlations \bar{c}_1 and \bar{c}_2 satisfy the equations

$$\bar{q} = (2\gamma_1 a_1 + 6\gamma_2 a_2 + 8\gamma_3 a_3 + 12\gamma_4 a_4 + 4\gamma_5 a_5 + 6\gamma_6 a_6 + 4\gamma_7 a_7 + 2\gamma_8 a_8 + 4\gamma_9 a_9 + 4\gamma_{10} a_{10} + 2\gamma_{11} a_{11})/W_0,$$

$$\bar{c}_1 = (2\gamma_1 a_1 + 4\gamma_2 a_2 + 2\gamma_5 a_5 - 4\gamma_6 a_6 - 2\gamma_9 a_9 - 2\gamma_{11} a_{11})/W_0, \quad (4.7)$$

$$\bar{c}_2 = (2\gamma_1 a_1 + 4\gamma_2 a_2 + 8\gamma_3 a_3 + 8\gamma_4 a_4 + 2\gamma_5 a_5 + 4\gamma_6 a_6 + 2\gamma_9 a_9 + 4\gamma_{10} a_{10} + 2\gamma_{11} a_{11})/W_0.$$

In particular, in the limit $D \rightarrow -\infty$, corresponding to the Ising model with a plaquette interaction, the critical line is given by

$$\frac{G}{J} = \frac{1}{2\beta J} \ln \frac{2e^{2\beta J}}{(e^{2\beta J} - 1)(2e^{2\beta J} - 1)}. \quad (4.8)$$

It can be checked that one has always $G/J > -1$, with G/J tending to the limit value -1 for vanishing temperature, and that our result is in good agreement with a previous transfer-matrix study by Nightingale.³¹ Furthermore, for $G/J = 0$ one recovers $\exp(2\beta J) = (5 + \sqrt{17})/4$, as in Ref. 28.

V. TEMPERATURE PHASE DIAGRAM

In the present section we shall present and discuss the results we have obtained for the finite-temperature phase diagram, paying particular attention to the effects of the plaquette interaction term.

As a first step we shall investigate the modifications occurring in the BEG model ferromagnetic-paramagnetic transition as the plaquette interaction is introduced, for the range of K/J values considered in Refs. 9,20 (as we said above, we do not consider here the antiquadrupolar phase).

A general feature is that a positive G enhances the ferromagnetic long-range order, increasing the corresponding transition temperature, and vice versa for negative G . In some cases a negative plaquette interaction induces a reentrant behavior which was not found for $G = 0$. It is also noteworthy that, for $G = 0$ and $K/J = -1$, we do not find a reentrant behavior, in agreement with renormalization group and in contrast with mean field theory.²⁰

Let us now turn our attention to the situations in which, for negative enough G/J , the S , A , and E ground states appear. We shall take $K/J = -1$, corresponding to the ground state depicted in Fig. 4 (indeed $K/J = -1$ is at the border between this situation and the one of Fig. 5, so that the region occupied by the Q state has width 0 and the topology turns out to be that of Fig. 4), and progressively decrease G/J in order to analyze all the possible combinations of ground states.

For $G/J = -0.90$ the ground state changes, as $D/4J$ increases, from F to E and then to P and the corresponding finite-temperature phase diagram is reported in Fig. 6(a). The E ground state turns into a ferrimagnetic phase at finite temperature, which has been denoted by I . This phase is rather peculiar since it is characterized by the relation $m_i = m_j < m_k = m_l$ (and the same for q); that is, two of the four sublattices (a nearest-neighbor pair, say, i and j) have large values of the order parameters, which saturate to 1 at low temperatures, while the other two have smaller order parameters, which tend to $1/2$ as the temperature vanishes. It

turns out that the lattice is divided in lines of spins with alternatively high and low values of the order parameters. In the case of Fig. 6(a) the ferrimagnetic and paramagnetic phases are completely separated by the ferromagnetic phase (except at zero temperature, of course), but this does not hold true in general, as can be seen in Fig. 6(b), where a first-order I/P transition appears at low temperature.

When $G/J = -1.50$ the ground states follow, for increasing $D/4J$, in the order S , A , E , P and the phase diagram is reported in Fig. 7(a). The A and E ground states turn into the same ferrimagnetic phase I , with no finite-temperature transition between them, but only a zero-temperature transition point which is indicated by an arrow in Fig. 7(a). On the left of this phase there is a low-temperature second-order phase transition between the S and P phases. A similar phase diagram (without a direct I/P transition) is found for the Blume-Capel model with plaquette interaction and shown in Fig. 7(b), and the S/P transition temperature tends to zero in the limit $D/4J \rightarrow -\infty$, in agreement with Eq. (4.8).

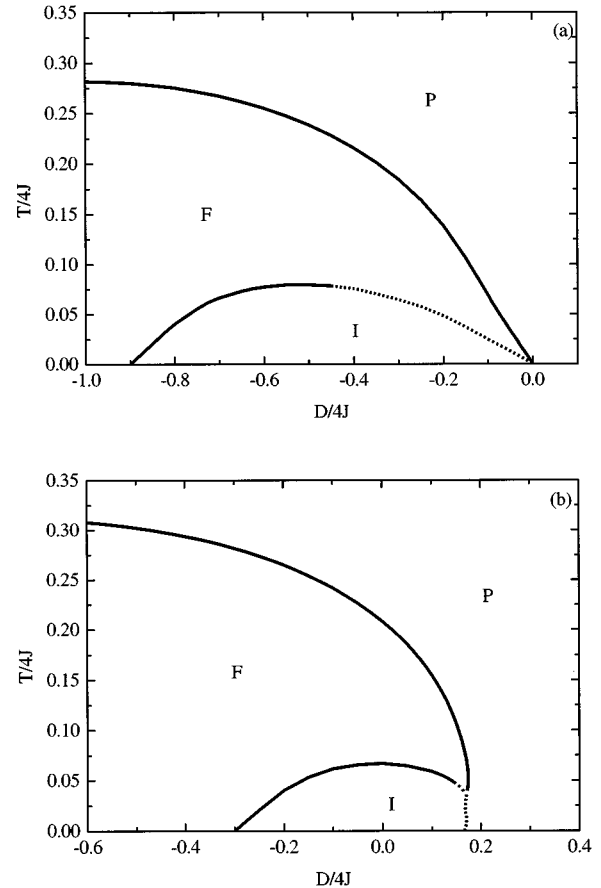


FIG. 6. Phase diagram for $K/J = -1.00$, $G/J = -0.90$ (a) and $K/J = -0.50$, $G/J = -0.80$ (b).

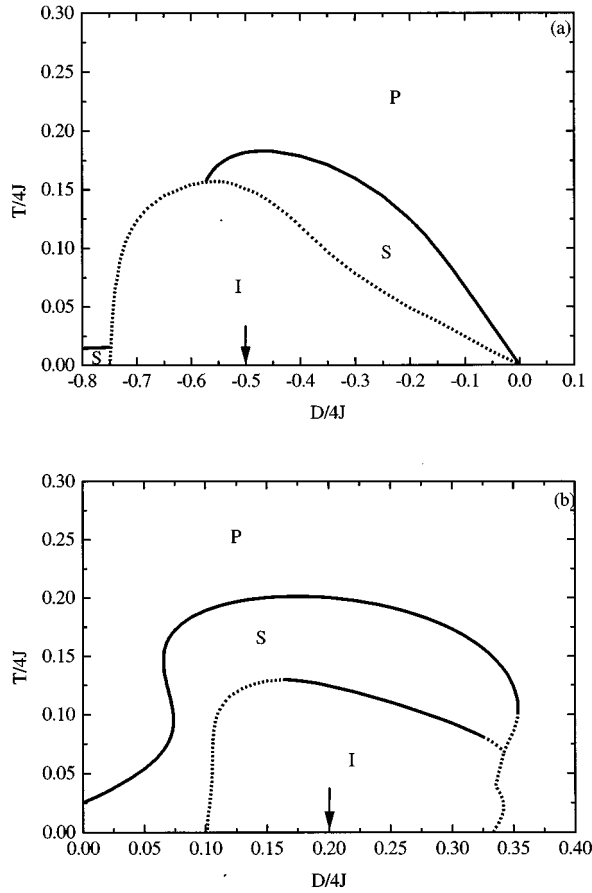


FIG. 7. Phase diagram for $K/J = -1.00$, $G/J = -1.50$ (a) and $K/J = 0$, $G/J = -1.20$ (b). The arrows indicate the zero-temperature transition points between A and E ground states.

Decreasing further G/J we have considered the case $G/J = -2.10$, when the sequence of ground states is S , A , P , obtaining the phase diagram reported in Fig. 8. It is very simple, with only a first-order transition separating the ferrimagnetic and paramagnetic phases. A low-temperature second-order S/P transition should occur on the left side of the phase diagram, but it is not found numerically, perhaps because the transition temperature is too low.

Notice also that a common feature of all the phase diagrams discussed above is the presence of several multicritical

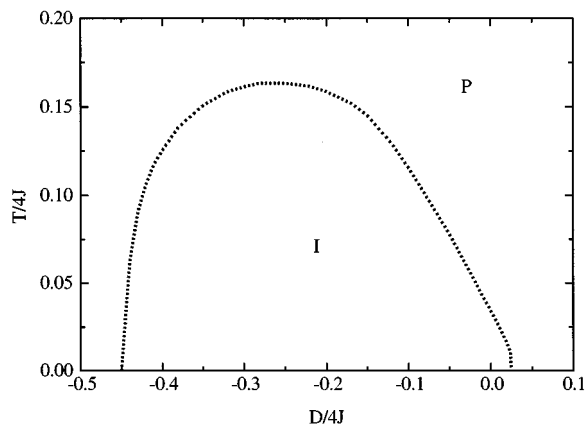


FIG. 8. Phase diagram for $K/J = -1.00$, $G/J = -2.10$.

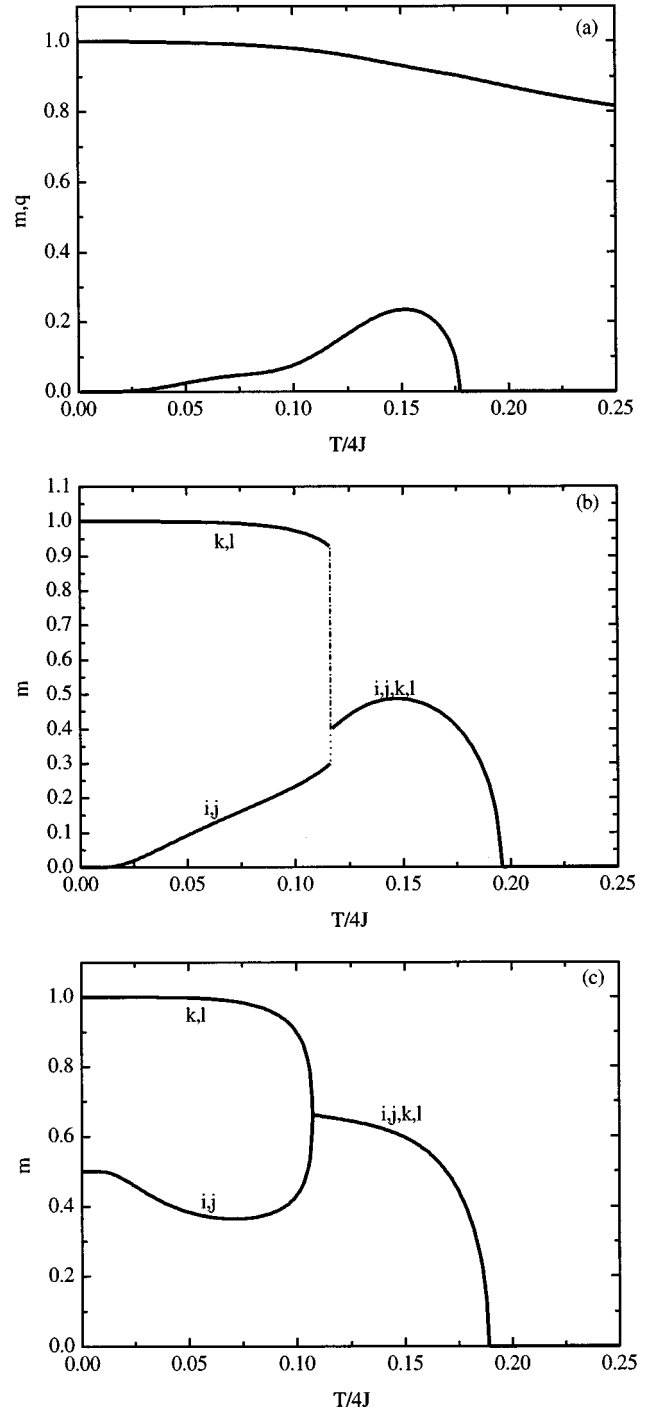


FIG. 9. Order parameters m and q vs temperature for $K/J = 0$, $G/J = -1.20$, and $D/4J = 0.08$ (a), 0.12 (b), and 0.26 (c). Letters indicate sublattices.

points and reentrant transition lines.

In order to better understand the new phases that we have obtained, it is useful to look at how the order parameters behave as the temperature varies. Figure 9 refers to the phase diagram in Fig. 7(b) and has been obtained for a sequence of increasing values of $D/4J$. In Fig. 9(a) we have a second-order transition from the S phase, characterized by sublattice invariance and weak ferromagnetic long-range order with a vanishing (as temperature vanishes) dipolar order parameter, into the paramagnetic phase. Increasing $D/4J$ the

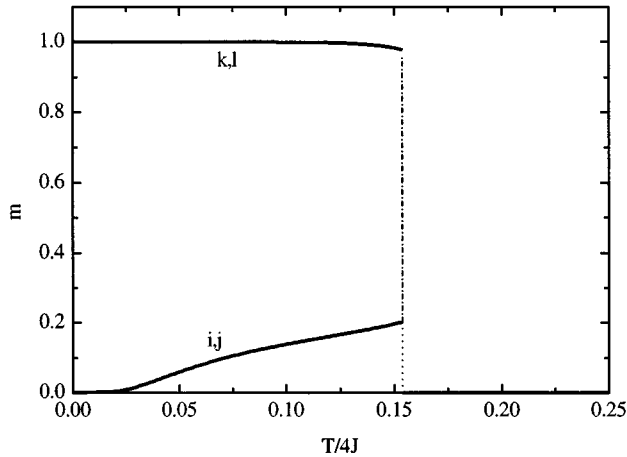


FIG. 10. Order parameters vs temperature for $K/J = -1.00$, $G/J = -1.50$, and $D/4J = -0.60$.

ground state becomes A , with [Fig. 9(b)] breaking of the sublattice invariance. At low temperatures the dipolar order parameter vanishes in two of the four sublattices and saturates in the remaining two, giving rise to the ferrimagnetic phase I . By further increasing $D/4J$ [Fig. 9(c)] we have still the ferrimagnetic phase I at low temperatures, but the ground state is now E : the dipolar order parameter saturates in two

of the four sublattices and tends to $1/2$ in the remaining two. Finally, a direct, first-order transition from the I (with ground state A) to the P phase is reported in Fig. 10, which refers to the phase diagram given in Fig. 7(a).

VI. CONCLUSIONS

We have studied the square lattice Blume-Emery-Griffiths model with a plaquette interaction, using the square approximation of the cluster variation method. After a detailed study of the ground state, which for negative plaquette interaction exhibits several new frustrated phases, equations for the ferromagnetic-paramagnetic critical temperature have been derived and the finite-temperature phase diagram has been discussed, making comparisons with the ordinary BEG model and with a previous result on the Ising model with plaquette interaction.

The frustrated ground states evolve at finite temperature in a homogeneous phase S with weak ferromagnetic long-range order and in a ferrimagnetic phase I , and the phase diagram exhibits a quite rich structure, with several multicritical points.

ACKNOWLEDGMENTS

One of us (L.R.E.) thanks INFM (Italy) and CAPES (Brazil) for financial support, and the Politecnico di Torino for kind hospitality.

- ¹M. Blume, V. J. Emery, and R. B. Griffiths, *Phys. Rev. A* **4**, 1071 (1971).
- ²J. Lajzerowicz and J. Sivardière, *Phys. Rev. A* **11**, 2079 (1975); J. Sivardière and J. Lajzerowicz, *ibid.* **11**, 2090 (1975); **11**, 2101 (1975).
- ³M. Schick and W. H. Shih, *Phys. Rev. B* **34**, 1797 (1986).
- ⁴K. E. Newmann and J. D. Dow, *Phys. Rev. B* **27**, 7495 (1983).
- ⁵S. A. Kivelson, V. J. Emery, and H. Q. Lin, *Phys. Rev. B* **42**, 6523 (1990).
- ⁶C. Buzano and L. R. Evangelista, *Liq. Cryst.* **14**, 1209 (1993).
- ⁷D. Furman, S. Dattagupta, and R. B. Griffiths, *Phys. Rev. B* **15**, 441 (1977).
- ⁸D. Mukamel and M. Blume, *Phys. Rev. A* **10**, 619 (1974).
- ⁹W. Hoston and A. N. Berker, *Phys. Rev. Lett.* **67**, 1027 (1991).
- ¹⁰D. M. Saul, M. Wortis, and D. Stauffer, *Phys. Rev. B* **9**, 4964 (1974).
- ¹¹Y. L. Wang and C. Wentworth, *J. Appl. Phys.* **61**, 4411 (1987).
- ¹²Y. L. Wang, F. Lee, and J. D. Kimel, *Phys. Rev. B* **36**, 8945 (1987).
- ¹³T. W. Burkhardt, *Phys. Rev. B* **14**, 1196 (1976).
- ¹⁴T. W. Burkhardt and H. J. Knops, *Phys. Rev. B* **15**, 1602 (1977).
- ¹⁵A. N. Berker and M. Wortis, *Phys. Rev. B* **14**, 4946 (1976).
- ¹⁶M. Kaufman, R. B. Griffiths, J. M. Yeomans, and M. E. Fisher, *Phys. Rev. B* **23**, 3448 (1981).
- ¹⁷R. R. Netz and A. N. Berker, *Phys. Rev. B* **47**, 15 019 (1993).
- ¹⁸O. F. de Alcantara Bonfim and F. C. Sá Barreto, *Phys. Lett. A* **109**, 341 (1985).
- ¹⁹F. C. Sá Barreto, *Rev. Bras. Fis.* **20**, 152 (1990).
- ²⁰W. Hoston and A. N. Berker, *J. Appl. Phys.* **70**, 6101 (1991).
- ²¹K. G. Chakraborty, *J. Phys. C* **21**, 2911 (1988).
- ²²T. Kaneyoshi and E. F. Sarmiento, *Physica A* **152**, 343 (1988).
- ²³T. Kaneyoshi, *Physica A* **164**, 730 (1990).
- ²⁴C. Buzano and L. R. Evangelista, *J. Magn. Magn. Mater.* **104**, 231 (1992).
- ²⁵A. Rosengren and S. Lapinskas, *Phys. Rev. Lett.* **71**, 165 (1993).
- ²⁶C. Buzano and L. R. Evangelista, *Int. J. Mod. Phys. B* **7**, 1259 (1993).
- ²⁷C. Buzano and A. Pelizzola, *Physica A* **189**, 333 (1992).
- ²⁸R. Kikuchi, *Phys. Rev.* **81**, 988 (1951).
- ²⁹G. An, *J. Stat. Phys.* **52**, 727 (1988).
- ³⁰T. Morita, *J. Stat. Phys.* **59**, 819 (1990).
- ³¹M. P. Nightingale, *Phys. Lett. A* **59**, 486 (1976).
- ³²M. Blume, *Phys. Rev.* **141**, 517 (1966).
- ³³H. W. Capel, *Physica* **32**, 966 (1966).
- ³⁴R. Kikuchi, *J. Chem. Phys.* **60**, 1071 (1974).